SUPPLEMENT TO THE *WELDING JOURNAL*, SEPTEMBER 2009
Sponsored by the American Welding Society and the Welding Research Council

Crack-Free Electron Beam Welding of Allvac 718Plus® Superalloy

Careful control of preweld heat treatment and cooling rates was found to siginificantly reduce HAZ cracking

BY O. A. IDOWU, O. A. OJO, AND M. C. CHATURVEDI

ABSTRACT

Allvac 718Plus® was welded in different preweld heat-treated conditions in order to investigate the effects of preweld heat treatments on its cracking behavior during welding. The occurrence of HAZ cracking in the alloy was found to be closely related to grain boundary boron segregation and variation in grain size, both of which were controlled by preweld heat treatments. It was demonstrated that crack-free welds of the alloy can be made by a proper selection of preweld heat treatment.

Introduction

Allvac 718Plus® is a newly developed γ'— strengthened-nickel-based superalloy. It was developed by ATI Allvac (Ref. 1) as a derivative of the widely used Inconel® 718 superalloy. The alloy was developed to overcome service temperature limitations that are usually encountered with components made with 718. Alloy 718 loses its strength above 650°C due to instability of its main strengthening phase, γ''. Above this temperature, the $D0_{22}$ ordered body -centered tetragonal phase of γ'' becomes unstable and transforms to an equilibrium delta (δ) phase with orthorhombic (D0a) crystal structure with a plate-like morphology, which impairs its high-temperature mechanical properties. In developing 718Plus, major compositional changes, which are detailed in the work of Cao et al. (Ref. 2), were made to its principal alloy, 718. These changes resulted in a change in the main strengthening phase of 718Plus from γ'' to γ' phase that is known to be more stable at high temperatures and thus improves the strength of the superalloy. Thus, it is claimed (Ref. 2) that hot-section components of both aero-engine and land-based power-generation turbines made of 718Plus superalloy can operate at temperatures up to 55°C higher than those made of 718.

Although 718Plus can withstand high service temperatures, recent studies on its weldability (Refs. 3, 4) have shown that it is susceptible to heat-affected zone (HAZ) cracking during high-power beam welding, a problem that plagues many other nickel-based superalloys. It is known that HAZ cracking during welding of superalloys can be significantly reduced or eliminated by the use of appropriate preweld heat treatments (Ref. 5). Therefore, the aim of the present work was to investigate the influence of preweld heat treatments on the cracking behavior of 718Plus. Ultimately, a preweld heat treatment schedule that would be capable of preventing the occurrence of HAZ cracking during welding was sought.

KEYWORDS

Allvac 718Plus®
Inconel® 718
Superalloy
Boron
Grain Boundary Segregation
Grain Size
SIMS Analysis
Microstructural Analysis
Heat Treatment
Electron Beam Welding
Weld HAZ Cracking

O. A. IDOWU, O. A. OJO, and M. C. CHATURVEDI are with the Department of Mechanical and Manufacturing Engineering, University of Manitoba, Winnipeg, Manitoba, Canada.

Experimental Procedures

Materials and Preweld Heat Treatments

The 718Plus superalloy used in this study was supplied by ATI Allvac in the form of 305 × 127 × 16 mm hot rolled plate. The alloy contained about 30 ppm of boron, and the rest of its elemental composition is given in Table 1. Rectangular sections measuring 12 × 12 × 100 mm and 3 × 3 × 2 mm were cut normal to the rolling direction of the plate, and then solution heat treated for 1 h in an argon atmosphere in a furnace at 950°, 1050°, and 1150°C. The heat-treated coupons were cooled from the solution heat-treatment temperatures at various rates ranging from iced-water quenching (≈500°C/s), air cooling (≈25°C/s), to furnace cooling (≈0.25°C/s), as shown in Table 2.

SIMS Analysis

The SIMS technique was used to analyze grain boundary distribution of boron in this study. In the SIMS (Refs. 5, 6), a solid sample is bombarded with primary ions of few keV energy. This results in the sputtering of atomic species from the surface of the sample. Fractions of the species are emitted as negative, neutral, or positive secondary ions and their mass are analyzed in a mass spectrometer to determine the elemental, molecular, or isotopic composition of the surface. Due to the extremely high signal/background ratio of the mass spectrometer, SIMS can detect trace amounts of elements on a surface. It provides ion images with spatial resolution of a few μm and elemental resolution to a few ppm. The primary ion beam species used in SIMS include Cs^+, O_2^+, O^-, Ar^+, Ga^+, and Xe^+. Very electronegative elements such as H, O, S, and P are most sensitive to Cs^+ beam, while O_2^+ is used for most other elements.

In preparation for SIMS analysis in this

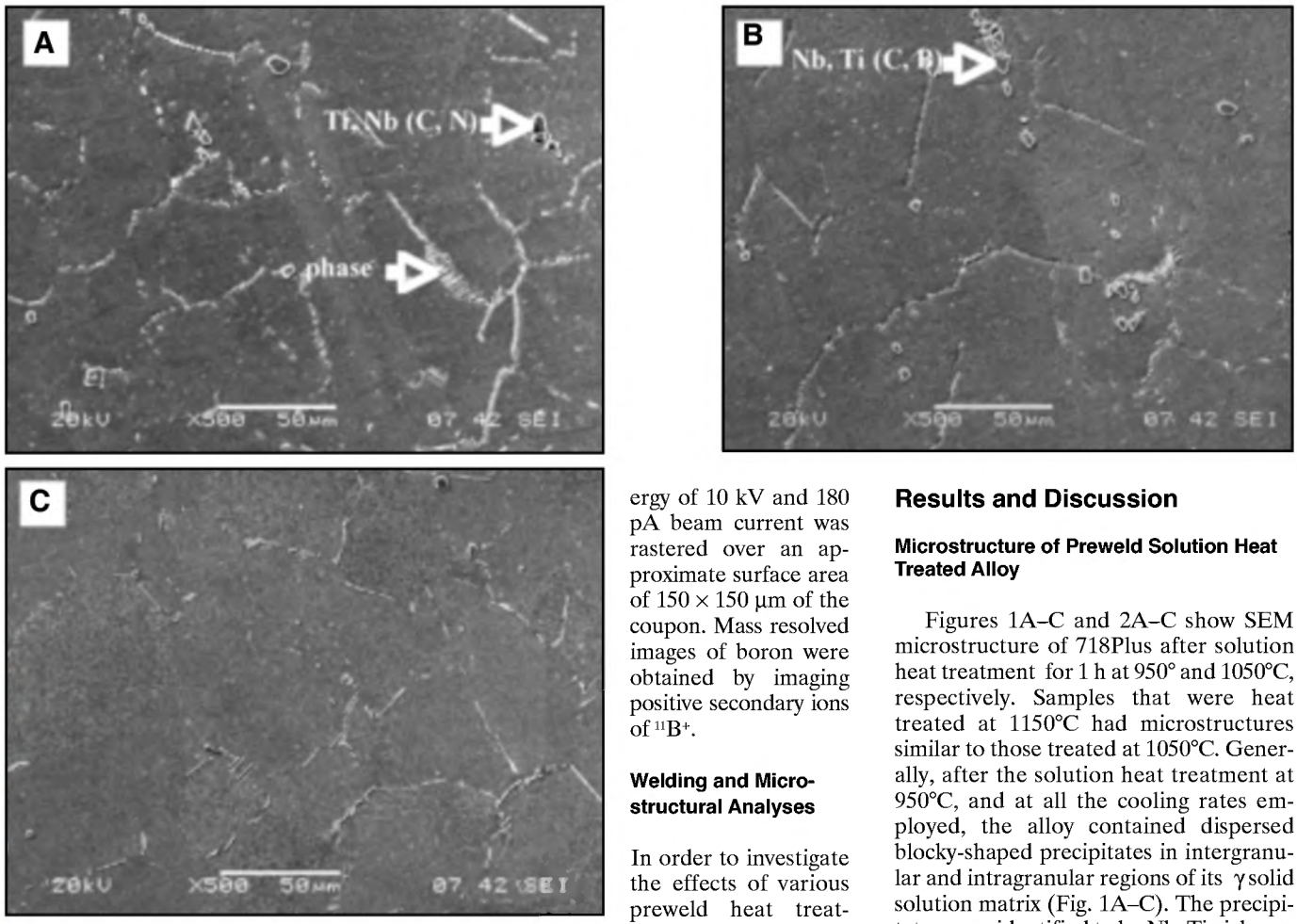

Fig. 1 — SEM microstructure of 718Plus solution heat treated at 950°C. A — Iced-water quenched; B — air cooled; C — furnace cooled. The top-right inset on 1C shows γ′ particles in γ matrix of the furnace-cooled samples.

study, 3 × 3 × 2 mm preweld heat-treated coupons were mounted in an epoxy base resin and polished to 1-µm finish using standard metallographic techniques. Thereafter, they were electro-etched in 10% oxalic acid at 6 V for 5 s. This revealed the grain boundaries, which were the areas of interest for SIMS analyses. A Vickers microhardness indenter was used to mark the grain boundaries, and the coupons were repolished to remove the etched surface layer while leaving the indentations. Finally, the coupons were removed from the epoxy base resin in which they were mounted. The coupons were then examined for grain boundary segregation of boron using a Cameca IMS-7f magnetic sector secondary ion mass spectrometer. The equipment was operated in a scanning microprobe mode. A primary ion beam of O_2^+ with impact energy of 10 kV and 180 pA beam current was rastered over an approximate surface area of 150 × 150 µm of the coupon. Mass resolved images of boron were obtained by imaging positive secondary ions of $^{11}B^+$.

Welding and Microstructural Analyses

In order to investigate the effects of various preweld heat treatments on HAZ cracking of 718Plus during welding, the 12 × 12 × 100 mm heat-treated specimens were welded autogenously along the 100 mm length using a focused electron beam at 44 kV voltage, 79 mA beam current, and 152 cm/min welding speed. Transverse sections of the welds were cut by electrodischarge machining and prepared by standard metallographic polishing technique for microstructural study. Thereafter, the specimens were etched electrolytically at 6 V for 5 s in a solution of 10% oxalic acid. Microstructures of preweld heat-treated and welded specimens were examined using an optical microscope and a JEOL 5900 scanning electron microscope (SEM) in both secondary and backscattered electron (BSE) imaging modes. The susceptibility of 718Plus to weld HAZ cracking was evaluated by measuring total length of cracks (TCL) observed in 8 sections of each weld.

Results and Discussion

Microstructure of Preweld Solution Heat Treated Alloy

Figures 1A–C and 2A–C show SEM microstructure of 718Plus after solution heat treatment for 1 h at 950° and 1050°C, respectively. Samples that were heat treated at 1150°C had microstructures similar to those treated at 1050°C. Generally, after the solution heat treatment at 950°C, and at all the cooling rates employed, the alloy contained dispersed blocky-shaped precipitates in intergranular and intragranular regions of its γ solid solution matrix (Fig. 1A–C). The precipitates were identified to be Nb, Ti-rich carboborides and Ti, Nb-rich carbonitrides which are the primary solidification constituents of the alloy (Ref. 3). Also, grain boundary regions of the alloy were outlined by secondary precipitates of δ phase having platelet or blocky morphology. In addition to the carbides and δ phase, precipitates of γ′ particles were observed within the γ matrix of the furnace-cooled samples. A high-magnification SEM image showing spherical-shaped γ′ particles is shown in the top-right inset of Fig. 1C. The γ′particles precipitated from γ matrix during continuous cooling of 718Plus in the furnace at a slow rate (≈ 0.25°C/s). Specimens heat treated at 1050° and 1150°C contained microconstituents similar to those observed in the samples that were heat treated at 950°C, with the exemption of δ phase. δ-phase precipitates were not observed after the solution treatments at 1050° and 1150°C because these temperatures are above the solvus of δ phase in 718Plus, which has been reported

Table 1 — Bulk Chemical Composition (wt-%) of 718Plus

Ni	Cr	Fe	Co	Nb	Mo	Al	W	Ti	Mn	C	Si	V	P	B	Mg	S
Bal	17.92	9.33	9.00	5.51	2.68	1.50	1.04	0.74	0.03	0.022	0.02	0.02	0.006	0.003	0.0008	0.0003

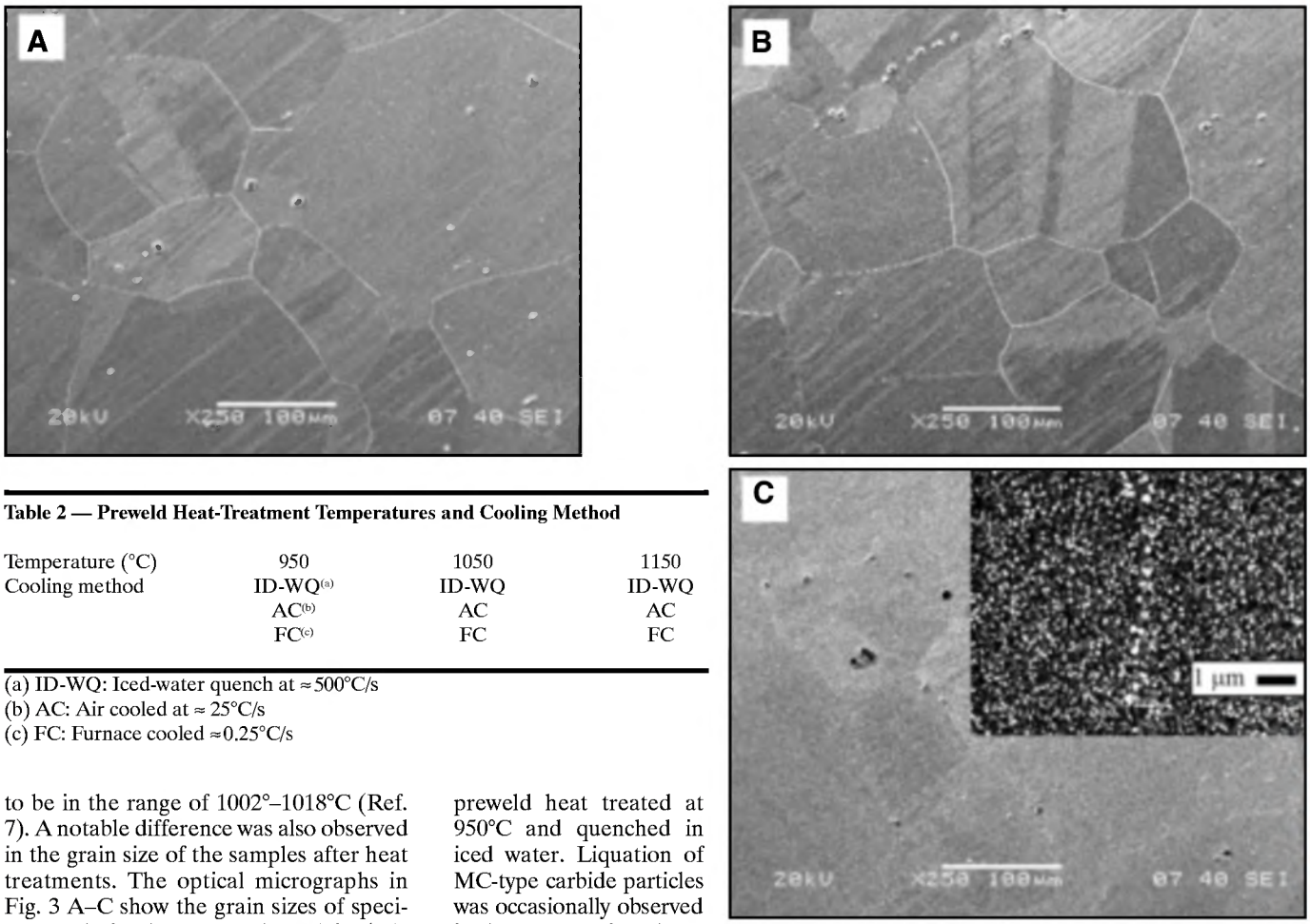

Fig. 2 — SEM microstructure of 718Plus solution heat treated at 1050°C. A — Iced-water quenched; B — air cooled; C — furnace cooled. The top-right inset on 1C shows γ′ particles in γ matrix of furnace-cooled samples.

Table 2 — Preweld Heat-Treatment Temperatures and Cooling Method

Temperature (°C)	950	1050	1150
Cooling method	ID-WQ[a]	ID-WQ	ID-WQ
	AC[b]	AC	AC
	FC[c]	FC	FC

(a) ID-WQ: Iced-water quench at ≈500°C/s
(b) AC: Air cooled at ≈ 25°C/s
(c) FC: Furnace cooled ≈0.25°C/s

to be in the range of 1002°–1018°C (Ref. 7). A notable difference was also observed in the grain size of the samples after heat treatments. The optical micrographs in Fig. 3 A–C show the grain sizes of specimens solution heat treated at 950°C (≈58 µm grain size), 1050°C (≈120 µm grain size), and 1150°C (≈360 µm grain size), respectively, and air cooled. The micrographs depict the variation in grain size of the alloy after these heat treatments. The approximate mean diameter of the grains after all the preweld solution heat treatments are presented graphically in Fig. 4. It is seen that no significant variation in grain size occurred with variation in cooling rate. However, the grain size increased approximately by a factor of two and six when heat treatment temperature was increased from 950° to 1050°C and 1150°C, respectively. The dramatic grain growth that occurred at 1050° and 1150°C can be attributed to the dissolution of δ-phase precipitates during heat treatments at these temperatures, as shown in Fig. 2. It is known that δ phase pins grain boundaries, and thereby prevents/limits grain growth during high-temperature exposure (Ref. 8). Thus, no significant grain growth occurred during the treatment at 950°C where the grain boundaries were outlined and successfully pinned by δ phase — Fig. 1.

HAZ Microstructure of Welded Alloy

The SEM backscattered electron (BSE) image in Fig. 5 shows weld HAZ microstructure of the specimen that was preweld heat treated at 950°C and quenched in iced water. Liquation of MC-type carbide particles was occasionally observed in the HAZ region closer to the fusion zone of the weld. Also, grain boundary liquation was observed in HAZ region up to about 250 µm from the fusion zone, but HAZ cracking was not observed. The samples that were preweld heat-treated at 950°C and air or furnace cooled were also crack free. Their HAZ microstructures were similar to those of the samples that were quenched in iced water — Fig. 5. However, SEM microstructures of the preweld and weld HAZ of the furnace-cooled sample (Fig. 6A, B) suggests that liquation of γ′ particles occurred in the heat-affected zone during welding. The underlying mechanism of the constitutional liquation of γ′ precipitates in γ′ strengthened nickel-based superalloys has been discussed in detail in the work of Ojo et al. (Refs. 9, 10). An explicit consideration of the potential effects of this on the weldability of 718Plus (in aged condition) is a subject of future work. However, it has been reported (Refs. 9, 10) that liquid film from constitutionally liquated γ′ precipitate can contribute to weld HAZ cracking if it penetrates and wets HAZ grain boundaries.

The weld HAZ microstructures of samples that were preweld heat treated at 1050° and 1150°C, respectively, were similar to those that were heat treated at 950°C. However, HAZ cracks were observed in the samples that were preweld heat treated at 1050° and 1150°C. Representative optical and SEM images of a cracked region is shown in Fig. 7A and B, respectively. As shown in the figures, the cracks were mostly present within the neck region of the nail-head-shaped welds. The degree of cracking in these samples was quantified by the measurement of total crack lengths (TCL) in them. The average value of TCL observed in variously heat treated material is shown in Fig. 8. It is seen that cracking was not observed in the welds in samples that were preweld heat treated at 950°C and cooled at the three cooling rates. However, as shown in Fig. 8, HAZ cracking occurred in the welds when the preweld heat treatment temperature was increased to 1050° and 1150°C. Figure 8 also shows that, at 1050° and 1150°C, the highest degree of cracking occurred in air-cooled samples. This was followed by furnace-cooled samples, while the lowest extent of cracking was found in samples that were quenched in iced water. At all the three cooling rates, the degree of

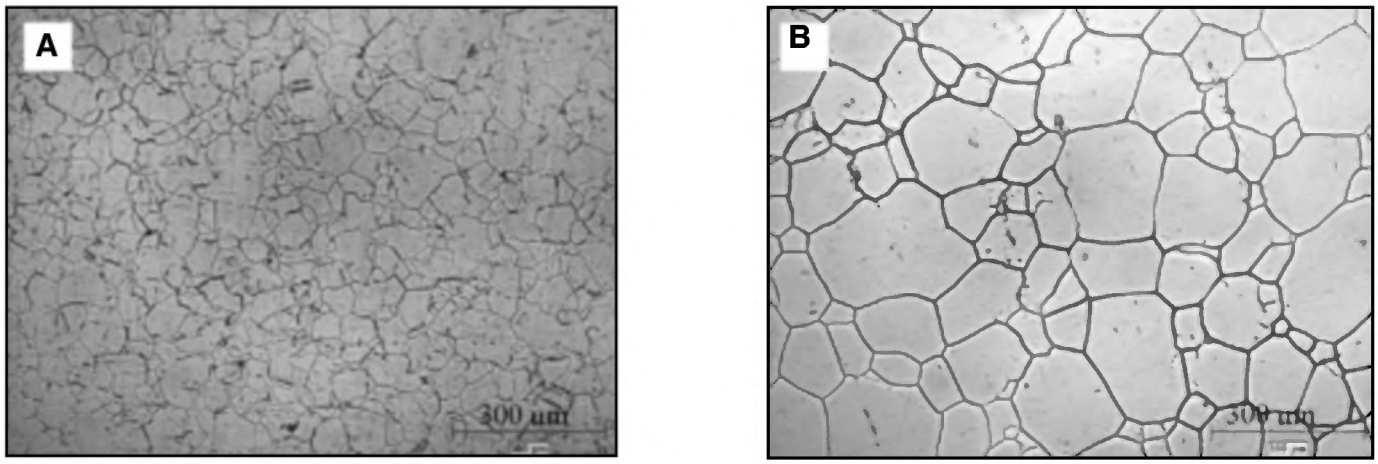

Fig. 3 — Optical micrographs (100×, 10% oxalic etch) of 718Plus showing the variation in grain size after solution heat treatment. A — At 950°C; B — at 1050°C; C — at 1150°C. All were followed by air cooling.

cracking was always higher in samples preweld heat treated at 1150°C compared to those that were heat treated at 1050°C. Although constitutional liquation of MC-type carbides was observed in this work, and has been reported to contribute to HAZ cracking in 718Plus (Ref. 11), a careful study of the variation of cracking with preweld heat-treatment temperature and cooling rate, which did not affect the volume fractions of constitutionally liquating MC-type carbides, suggested that cracking was more influenced by two main factors, viz., segregation of B and grain size of the material, which are discussed next.

Grain Boundary Segregation of Boron

The cause of intergranular cracking that often occurs in the HAZ of austenitic alloys during welding is generally attributed to a combination of mechanical driving force for cracking, threshold tensile welding stresses, and a crack susceptible microstructure such as with liquated grain boundaries. The liquation of a HAZ grain boundary during welding causes its solid-solid interfacial bond to be replaced by a weaker solid-liquid bond. Consequently, this reduces the threshold tensile welding stress that is required to cause the liquated grain boundary's decohesion. Thus, the inherent resistance of an alloy to HAZ cracking is reduced by liquation reaction. Grain boundary liquation can occur by either equilibrium supersolidus or nonequilibrium subsolidus melting. However, the mere occurrence of liquation reaction is not sufficient to produce a crack susceptible microstructure. It is essential that the liquid film penetrates and wets the grain boundaries and is stable over a wide range of temperatures to allow enough stresses to build up during weld cooling. The presence of positively partitioning elements (i.e., $k < 1$), particularly boron, enhances the wettability and increases the stability of grain boundary liquid film, and boron has been described as the most detrimental element causing grain boundary liquation cracking (Refs. 12–14), although it improves creep-rupture life of the alloy. Boron is particularly more detrimental as it has a tendency to preferentially segregate to grain boundaries during thermo mechanical processing of an alloy, or thermal treatments prior to welding.

The thermally induced grain boundary segregation of solute atoms, e.g., boron, is a diffusion controlled process that can occur by two mechanisms, viz., equilibrium segregation and nonequilibrium segregation. Equilibrium segregation occurs when a polycrystal is held at a sufficiently high temperature to permit appreciable diffusion of misfit impurity atoms within its grains to loosely packed interfaces, e.g., grain boundaries. The impurity atoms are absorbed by such interfaces in order to reduce their free energy (Ref. 15), and are thereby said to "segregate" to the interface. The extent of such equilibrium segregation is known to decrease with an increase in heat-treatment temperature, but is independent of cooling rates. On the other hand, thermally induced nonequilibrium segregation (Refs. 16, 17), as its name suggests, occurs under nonequilibrium thermal conditions, particularly when cooling from elevated temperatures over a range of cooling rates. This type of segregation has been widely described by a solute drag mechanism (Refs. 18, 19), which involves the following. During high-temperature annealing, an equilibrium concentration of vacancies is generated and distributed within the grain interior of a polycrystal. As the temperature decreases during cooling, the grains become supersaturated with vacancies. Since grain boundaries act as perfect sinks for point defects, a vacancy concentration gradient is set up between the supersaturated grains and the boundaries (Ref. 20). Consequently, vacancies diffuse down the concentration gradient to grain boundaries where they are annihilated. However, if some of the vacancies are attracted to impurity atoms, vacancy-solute complexes will be formed, and a proportion of the impurity atoms (those with positive vacancy-solute binding energies [Ref. 13]) will be dragged with vacancies toward grain boundaries. Thus, the grain boundaries will become gradually enriched with impurity solute atoms while the vacancies are being annihilated.

In contrast to equilibrium segregation, the degree of nonequilibrium segregation depends on cooling rates and vacancy-solute binding energy. The degree of nonequilibrium segregation increases with an increase in heat treatment temperature. The cooling rate is, however, very critical. If cooling rate is very rapid, sufficient time may not be available for a significant diffusion of complexes to grain boundaries to occur (Ref. 14). On the other hand, if the

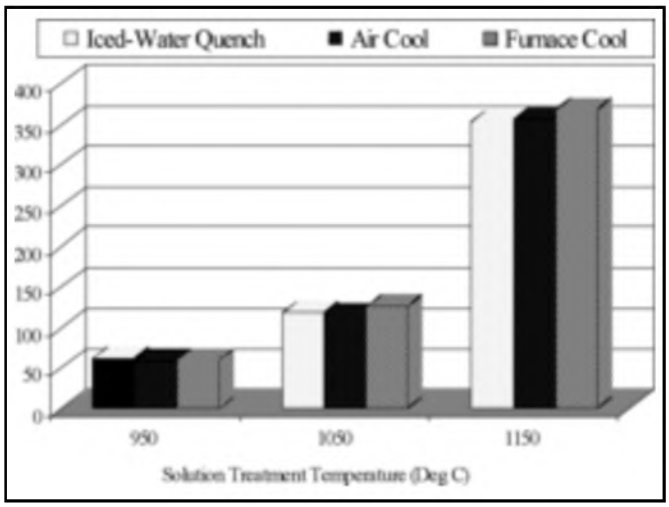

Fig. 4 — Variation in average grain size of 718Plus with preweld heat-treatment temperature and cooling rate.

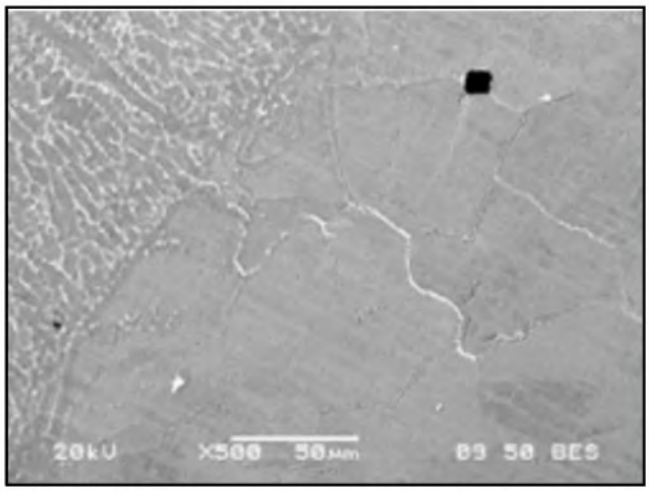

Fig. 5 — SEM micrograph showing the absence of HAZ cracking in the weld of 718Plus that was preweld solution heat treated at 950°C and iced-water quenched.

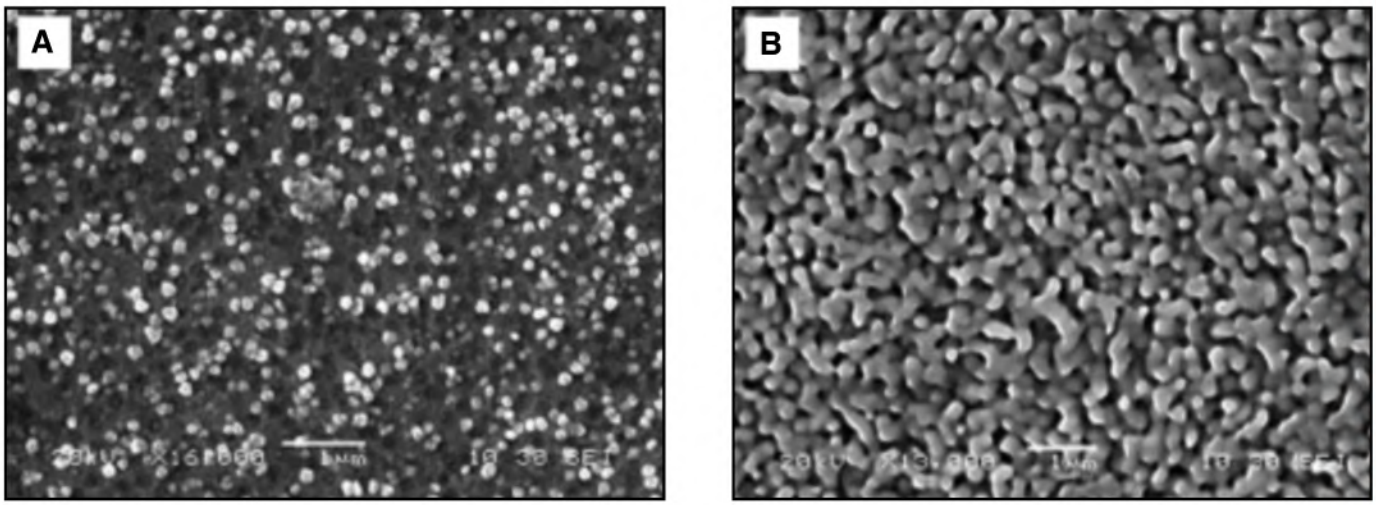

Fig. 6 — SEM micrographs showing γ′ particles. A — Before welding (i.e., after 950°C + furnace cool); B — after welding.

cooling rate is very slow, desegregation of solute atoms may occur. That is, segregated solute atoms on grain boundaries may diffuse away from their grain boundary sites back to grain interior when a solute concentration gradient occurs between the grain boundaries and the grain interior (Refs. 21, 22). Therefore, the degree of nonequilibrium segregation is usually highest at intermediate cooling rates when sufficient time is available to let vacancy-solute complexes diffuse to grain boundaries but is not sufficient to let the deposited solute atoms diffuse away from the grain boundary region.

Figures 9A–C to 11A–C show a set of SIMS images illustrating grain boundary distribution of boron in 718Plus after heat treatments at 950°, 1050°, and 1150°C at cooling rates corresponding to iced-water quench, air cool, and furnace cool. The images were recorded at the same instrumental settings of SIMS. Within the resolution limit of SIMS, boron segregation was significantly minimized in samples heat treated at 950°C, and cooled by any of the three cooling rates employed (Fig. 9 A–C). However, brighter boron signals, the degree of which varied with cooling rates and appeared to increase with heat-treatment temperature, were observed in samples heat treated at 1050° and 1150°C, respectively (Figs. 10A–C and 11A–C). The brightest boron intensity was observed in air-cooled samples while iced-water quenching and furnace cooling resulted in a significant reduction in the intensity. The intensities of boron signals could not be quantified by SIMS, thus, this work limits itself only to a qualitative comparison of the signals.

The dependence of nonequilibrium segregation on cooling rates suggests that the characteristically dynamic segregation pattern observed in the present work during preweld heat treatments of 718Plus, as shown in Figs. 9–11, is predominantly nonequilibrium in nature. It has been widely reported (Refs. 22, 23) that the segregation of boron to grain boundaries in austenitic steels occurs mainly during cooling from high temperatures and by nonequilibrium mechanism. Karlsson et al. (Ref. 24) used SIMS to study the nature of grain boundary segregation of boron in Type 316L austenitic stainless steel at heat treatment temperatures and cooling rates which ranged from 900° to 1250°C, and 530° to 0.25°C/s, respectively. They observed an increase in the degree of grain boundary segregation of boron when the cooling rate was decreased from 530° to 27°C/s. However, a further decrease in the cooling rate to 0.25°C/s resulted in desegregation of the boron atoms, an occurrence which was marked by a decrease in the intensity of boron atoms on the grain boundaries. In the present investigation, boron segregation was significantly minimized in 718Plus that was heat treated at 950°C and cooled at various rates (Fig. 9A–C), viz., iced-water quench (≈500°C/s), air cool (≈25°C/s), and furnace cool (≈0.25°C/s). However, boron segregated to grain boundaries when the heat-treatment

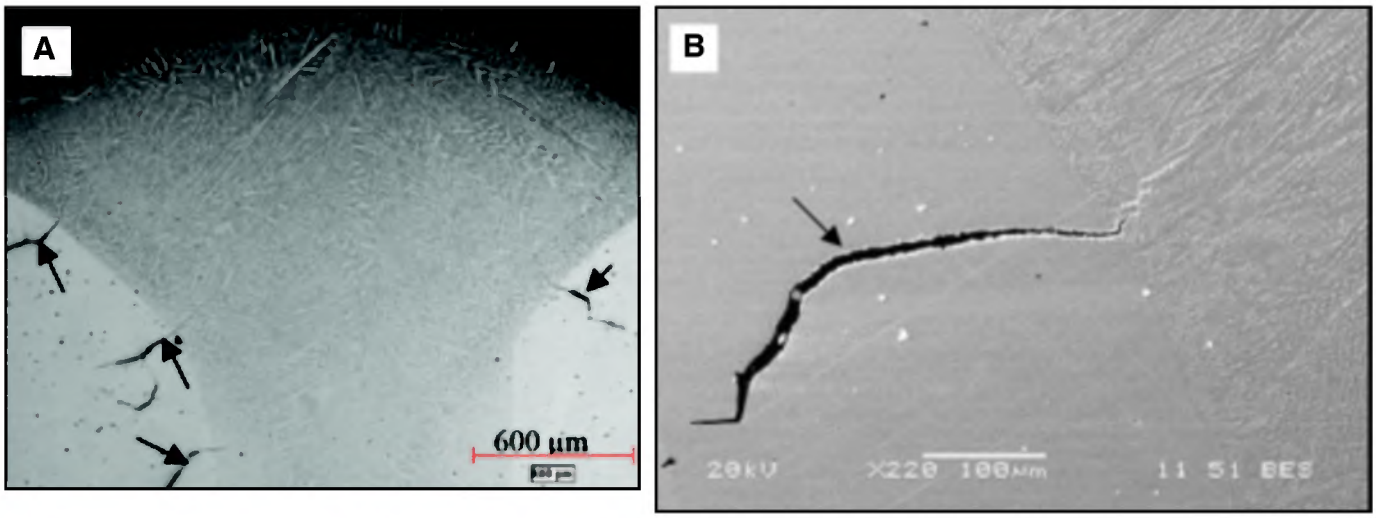

Fig. 7 — A — Optical; and B — SEM micrographs showing cracking in the weld HAZ of 718Plus that was preweld solution heat treated at 1150°C plus air cool.

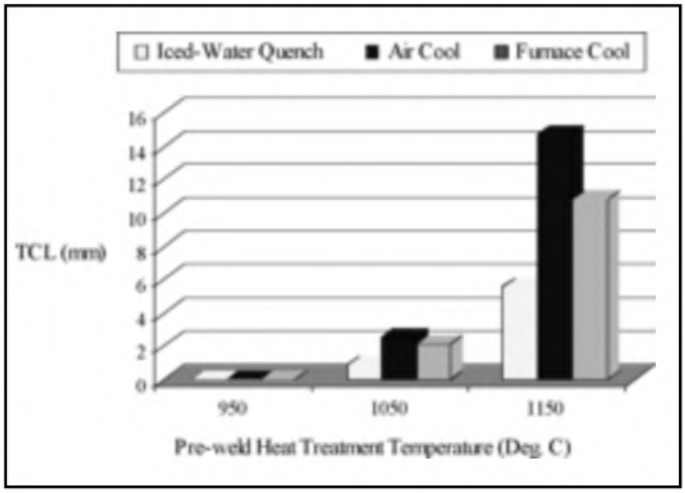

Fig. 8 — Variation in HAZ total crack length (TCL) of 718Plus with preweld heat-treatment temperature and cooling rate.

temperature was increased to 1050° and 1150°C, respectively. As shown in Figs. 10A–C and 11A–C at both temperatures, the degree of segregation varied with cooling rates. The brightest boron intensities were observed in samples that were cooled at the intermediate rate (air cool), while the fastest cooling rate (iced-water quench) resulted in an appreciable decrease in boron seregation. Moreover, desegregation of boron occurred during furnace cooling. A significant reduction in boron intensity was observed in furnace-cooled samples, although their intensities were always brighter than that observed in the iced-water quenched samples.

Boron is considered to be the most detrimental element causing grain boundary liquation cracking in Alloy 718 (Refs. 12–14), although cracking is also known to result from the constitutional liquation of MC-type carbides. Huang et al. (Refs. 13, 25) and Chen et al. (Ref. 26) evaluated the weldability of 718, in both cast and wrought forms, after the alloy was preweld treated using various heat treatment schedules that varied the degree of boron segregation on its grain boundaries. A close relationship was observed between the preweld heat treatments, the degree of boron segregation, and the susceptibility of 718 to HAZ cracking, which was evaluated by measuring the total crack length (TCL) that were observed in the HAZ. A heat treatment that increased boron segregation also increased cracking in the alloy and vice versa. In the present investigation, no cracking was observed in weld HAZ of the alloy, which was preweld heat treated at 950°C and cooled at various rates, which ranged from iced-water quench to furnace cool — Figs. 5, 8. SIMS analyses of the alloy in the preweld heat-treated conditions did not reveal a significant segregation of boron to its grain boundary regions either — Fig. 9. Evaluation of the welds that were preweld heat treated at 1050° and 1150°C, respectively, revealed that HAZ cracking occurred during welding — Figs. 7, 8. The degree of cracking (TCL) in the HAZ of the welds increased with an increase in the degree of boron segregation, which occurred on the grain boundaries of the alloy during the respective preweld heat treatments. As shown in Figs. 8, 10, and 11, iced-water quenching (fastest cooling rate) after preweld solution heat treatments at 1050° and 1150°C, respectively, resulted in the lowest degree of boron segregation and weld HAZ cracking. However, the highest degree of boron segregation and weld HAZ cracking were observed in air-cooled (intermediate cooling rate) coupons. In comparison to air cooling, the degree of HAZ microfissuring was reduced in coupons that were furnace cooled; a cooling condition where desegregation of boron from grain boundaries had started to occur and which reduced the amount of segregated boron on the grain boundaries.

To further confirm the contribution of boron to HAZ cracking in 718Plus, a version of the alloy that has a higher boron concentration (60 ppm of boron) was preweld heat treated for 1 h at 950°, 1050°, and 1150°C, respectively, and air cooled. Thereafter, the coupons were welded using the same electron beam welding conditions that were reported in the experimental technique section of this communication. SIMS images of segregated boron atoms on grain boundaries of the preweld heat-treated coupons, as well as the degree of HAZ cracking that occurred during their welding are shown in Figs. 12 and 13, respectively. Similar to the observations in the lower boron version (≈30 ppm) of 718Plus, boron segregation increased with an increase in preweld heat treatment temperature, and so did the weld HAZ cracking. However, it was noted that HAZ cracking was always higher in the higher boron version of 718Plus — Figs. 8, 13. Also, in contrast to the lower boron version of the alloy, a more significant grain boundary segregation of boron, accompanied by weld HAZ cracking was observed in the higher boron alloy, which was preweld heat treated at 950°C. In this heat treatment condition, grain boundary segregation was significantly reduced and no HAZ cracking was

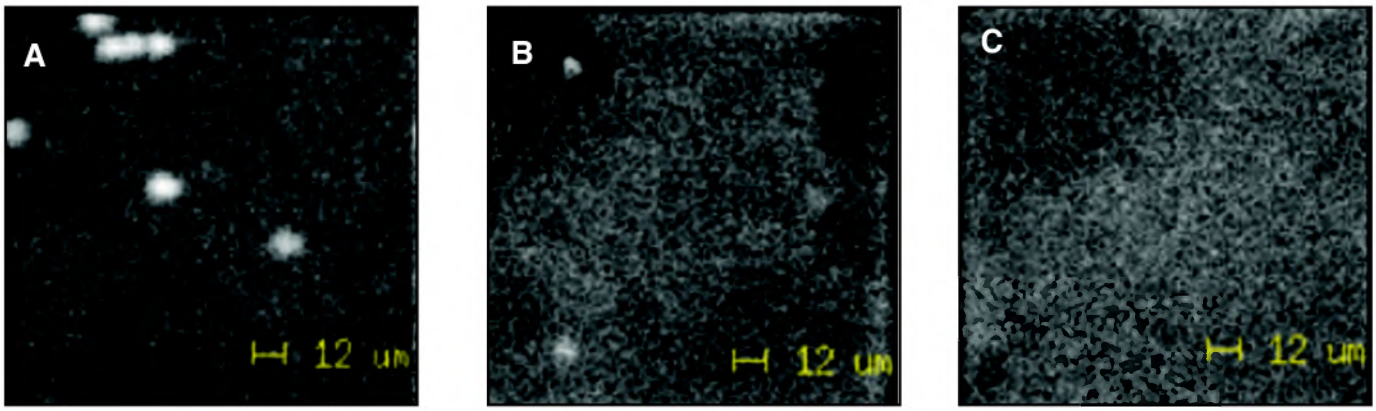

Fig. 9 — SIMS image of boron in 718Plus after heat treatment at 950°C. A — Iced-water quench; B — air cool; C — furnace cool.

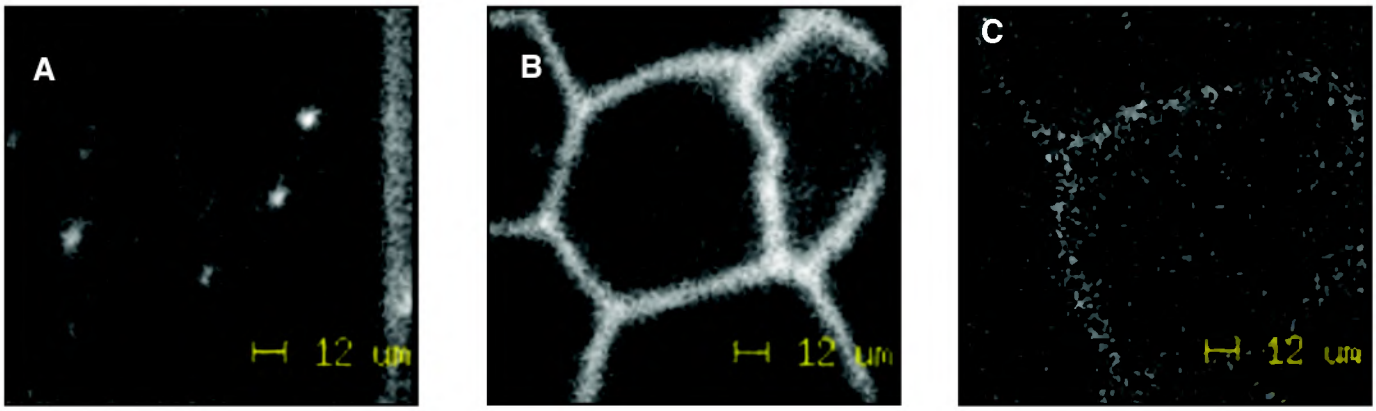

Fig. 10 — SIMS image of boron in 718Plus after heat treatment at 1050°C. A — Iced-water quench; B — air cool; C — furnace cool.

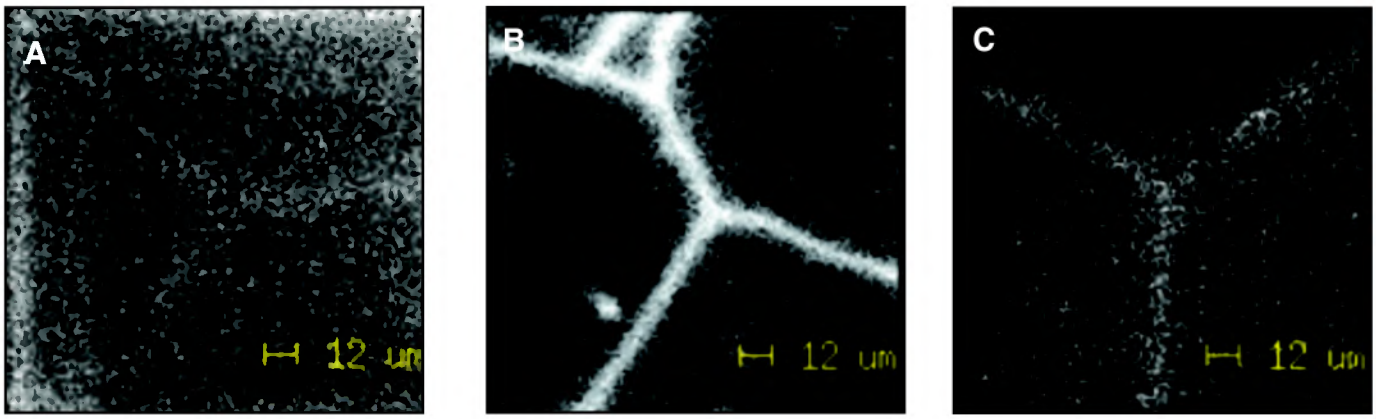

Fig. 11 — SIMS image of boron in 718Plus after heat treatment at 1150°C. A — Iced-water quench; B — air cool; C — furnace cool.

observed in the lower boron version of the alloy, as shown in Figs. 8 and 9. This further confirmed that boron played a significant role in causing HAZ cracking during welding of 718Plus. Therefore, its concentration should be as low as possible to improve the weldability of the alloy.

Generally, boron has been considered to influence the susceptibility of an alloy to weld HAZ cracking by the following mechanisms:

1) Segregated boron can act as a melting point depressant and reduce the melting temperature of grain boundary regions relative to surrounding matrix (Ref. 26).

2) Boron can extend the solidification range of liquid film on HAZ grain boundaries due to its low partition coefficient.

3) Boron can decrease solid-liquid interfacial energy (γ_{SL}) (Refs. 13, 27), which would enhance the wettability (and facilitate spreading) and/or increase the stability of grain boundary liquid during welding.

The existence of any or a combination of the above conditions, due to grain boundary boron segregation, which was observed in the present study, will increase the susceptibility of HAZ grain boundaries to liquation and facilitate spreading of the liquid film along the grain boundaries during welding. The inability of the liquated grain boundaries to support tensile stresses that develop during cooling of the welds will result in their cracking (Ref. 28), as observed in the present work

Preweld Grain Size

In addition to boron segregation, the variation in grain size of an alloy that takes place during preweld heat treatments can also affect the susceptibility of the alloy to

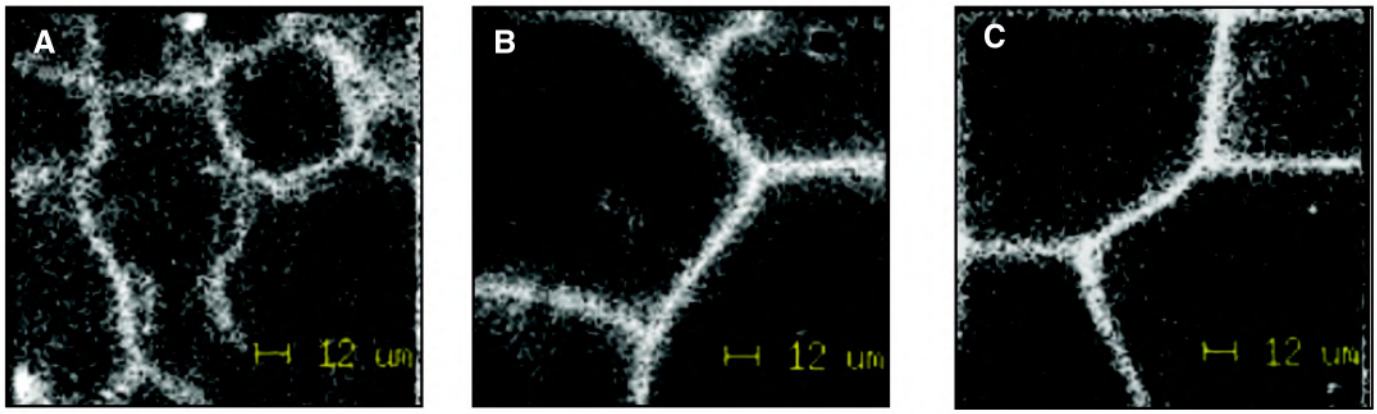

Fig. 12 — SIMS micrographs showing grain boundary boron segregation in 718Plus (higher boron version ≈ 60 ppm) after preweld heat treatment. A — At 950°C; B — at 1050°C; C — at 1150°C. All samples were air cooled.

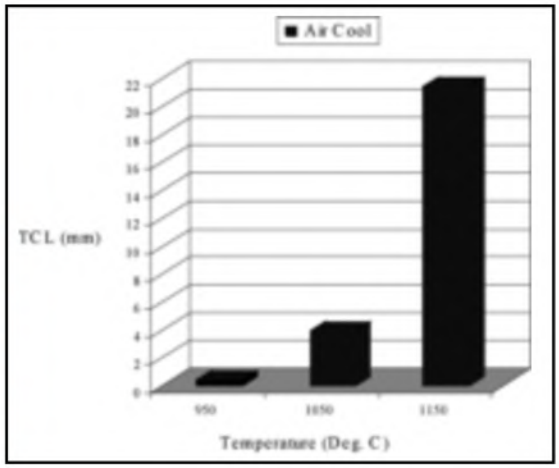

Fig. 13 — Variation in weld HAZ total crack length (TCL) of 718Plus (higher boron version ≈ 60 ppm) with preweld heat-treatment temperature. All samples were air cooled.

HAZ cracking during welding. Thompson et al. (Ref. 29) reported that HAZ cracking of Alloy 718 depends linearly on its grain size. It is a common knowledge that casting components are usually more prone to cracking than their wrought counterparts. This can be partly attributed to the usually larger grain sizes of the castings, apart from contributions from their segregated microstructure. Generally, the grain size of an alloy can also contribute to its weld HAZ cracking due to the following:

1) As predicted in the nonequilibrium grain boundary segregation model of Faulkner (Ref. 30), an increase in grain size could decrease total grain boundary surface area that is available for grain boundary segregation. Thus, provided heat treatment conditions are favorable for segregation to occur, an increase in the degree of boron segregation on the grain boundaries could arise, which could also increase their susceptibility to cracking during welding.

2) The grain size of an alloy can significantly influence the effectiveness of grain boundary liquid solidification by liquid film migration (LFM). This has been critically discussed in the work of Nakkalil et al. (Ref. 31) and will only be summarized here. Nakkalil et al. (Ref. 31) evaluated the occurrence of HAZ cracking in Incoloy® 903 that had a duplex grain structure. A considerable amount of microfissures was observed on the grain boundaries of a large-grained alloy. However, minimal cracking and an extensive occurrence of LFM were observed in the material with fine recrystallized grain boundaries. It was argued that an effective relief of the supersaturation of solutes in grain boundary liquid film by LFM can reduce the total solidification range of the liquid film. This can effectively reduce the susceptibility of an alloy to HAZ cracking. The velocity of LFM is dependent on grain boundary curvature, which has been reported (Ref. 32) to vary inversely with grain size. Thus, a fine-grained alloy should possess a substantial mean grain boundary curvature that would enhance the solidification of grain boundary liquid film by LFM and potentially reduce the susceptibility of the alloy to HAZ cracking.

3) When HAZ begins to accumulate strains due to welding stresses, grain boundary sliding is one mechanism that can operate to accommodate the strains (Ref. 33). However, this would increase stress concentrations at grain boundary triple points and could initiate microfissures. Once initiated, the microfissures can easily propagate along the liquated grain boundary regions. A large grain size would cause a longer interface sliding, which would lead to larger stress concentrations at grain boundary triple points (Ref. 29). This would increase the potential for crack initiation at grain boundary triple points, and therefore, liquation cracking.

In wrought alloy components, a significant increase in grain size will usually increase the susceptibility of the alloy to HAZ cracking during welding. In the present investigation, the grain size of 718Plus increased significantly with an increase in preweld solution heat-treatment temperatures ranging from 950° to 1150°C (Figs. 3, 4), and so was the susceptibility of the alloy to HAZ cracking — Fig. 8. For example, SEM observations of the welds of samples that were air cooled after preweld solution heat treatment at 950°C (this resulted in an average grain size ≈ 58 μm) revealed an absence of HAZ cracking — Fig. 5. However, significant HAZ cracking, the extent of which increased with temperature, occurred when the alloy was preweld solution heat treated at 1050° (≈ 120 μm grain size) and 1150°C (≈ 360 μm grain size), respectively.

A variation in weld HAZ cracking was also observed with cooling rates in samples that were preweld heat treated at 1050° and 1150°C — Fig. 8. This variation cannot be sufficiently explained with grain size considerations alone, since the grain size of the alloy did not vary appreciably with the cooling rates — Fig. 4. This suggests that though the size of the grains of 718Plus may have an effect on its susceptibility to HAZ cracking during welding, the cracking is however influenced by grain size and boron segregation. Therefore, it is concluded that both grain size and grain boundary segregation of boron contributed to the observed variation in HAZ cracking of 718Plus with temperatures and cooling rates.

Summary and Conclusions

1) Weld HAZ cracking in 718Plus was significantly influenced by preweld solution heat treatment temperature and cooling rate. No cracking was observed in samples that were heat treated at 950°C and cooled either by iced water quenching, air cooling, or furnace cooling. However, HAZ cracking occurred in samples that were preweld heat treated at 1050° and 1150°C, respectively. The degree of cracking in samples varied with cooling rates.

2) In samples that were preweld heat treated at 1050° and 1150°C, respectively, the highest degree of cracking occurred in air-cooled samples. This was followed by furnace-cooled samples, while the lowest degree of cracking was found in samples that were quenched in iced-water after preweld heat treatment. At all the three cooling rates, the degree of cracking was always higher in samples preweld heat treated at 1150°C than those that were solution treated at 1050°C.

3) The occurrence of weld HAZ cracking in 718Plus is concluded to be associated with nonequilibrium grain boundary segregation of boron which depended on the preweld solution heat-treatment temperature and cooling rates, and also the grain size of the alloy prior to welding, which was also dependent on the preweld treatment temperature.

4) It is concluded from this study that crack-free welds of 718Plus can be achieved by carrying out a preweld solution heat treatment at 950°C. At this temperature, both grain growth and nonequilibrium grain boundary segregation of boron were considerably minimized.

Acknowledgments

Financial support for this work was provided by the Natural Science and Engineering Research Council of Canada (NSERC) and is gratefully acknowledged. The authors would also like to thank Bristol Aerospace Ltd. in Winnipeg for welding the samples. One of the authors (O. A. Idowu) also acknowledges gratefully the awards of postgraduate scholarships by NSERC and the University of Manitoba. Thanks are also due to Dr. Rong Liu of the Department of Geological Sciences, University of Manitoba, for his technical assistance with SIMS analyses. Finally, we thank ATI Allvac for providing Allvac 718 Plus alloy.

References

1. Cao, W. D. 2004. U.S. Patent No.: 6,730.254 B2.
2. Cao, W. D., and Kennedy, R. L. 2004. *Superalloys 2004.* K. A. Green, T. M. Pollock, H. Harada, T. E. Howson, R. C. Reed, J. J. Schirra, S. Walston, eds. The Minerals, Metals and Materials Society, pp. 91–99.
3. Idowu, O. A., Ojo, O. A., and Chaturvedi, M. C. 2007. *Mater. Sci. Eng.* A 454–455, pp. 389–397.
4. Vishwakarma, K. R., and Chaturvedi, M. C. *Mater. Sci. Tech.* Article in Press.
5. Huang, X. 1994. PhD thesis, The University of Manitoba, pp. 1–295.
6. *Analysis Techniques: SIMS*, Cameca, *www.cameca.com*.
7. Cao, W. D. 2005. *Superalloys 718, 625, 706 and Derivatives.* E.A. Loria (ed.) The Minerals, Metals and Materials Society, pp. 165–177.
8. Donachie, M. J., and Donachie, S. J. 2002. *Superalloys — A Technical Guide*, 2nd ed., ASM International, pp. 225, 226.
9. Ojo, O. A., Richards, N. L., and Chaturvedi, M. C. 2004. *Scripta Materialia* 50: 641–646.
10. Ding, R. G., Ojo, O. A., and Chaturvedi, M. C. 2006. *Scripta Materialia* 56: 5.
11. Vishwakarma, K. R., and Chaturvedi, M. C. 2005. *Superalloys 718, 625, 706 and Derivatives*. E. A. Loria (ed.). The Minerals, Metals and Materials Society, pp. 637–647.
12. Kelly, T. J. 1989. *Welding Journal* 68: 44-s to 51-s.
13. Huang, X., Chaturvedi, M. C., and Richards, N. L. 1997. *Acta Mater.* 45: 3095–3107.
14. Chaturvedi, M. C. 2007. *Materials Science Forum* 546-549: 1163–1170.
15. McLean, D. 1957. *Grain Boundaries in Metals,* Oxford University Press, Oxford, UK.
16. Westbrook, J. H., and Aust, K. T. 1963. *Acta Mater.* 11: 1151.
17. Westbrook, J. H. 1964. *Metall. Rev.* 9: 415.
18. Faulkner, R. G. 1996. *Int. Mater. Rev.* 41: 198.
19. Tingdong, X., and Buyuan, C. 2004. *Prog. Mater. Sci.* 49: 109.
20. Faulkner, R. G., Jones, R. B., Lu, Z., and Flewitt, P. E. J. 2005. *Phil. Mag.* 85(19): 2065–2099.
21. He, X. L., Chu, Y. Y., and Jonas, J. J. 1989. *Acta. Metall.* 37(11): 2905–2916.
22. Chen, W., Chaturvedi, M. C., Richards, N. L., and McMahon, G. 1998. *Metall. Trans. A* 29A: 1947–1954.
23. Williams, T. M., Stoneham, A. M., and Harries, D. R. 1976. *Metal Science* 19: 14–19.
24. Karlsson, I., Norden, H., and Odelius, H. 1998. *Acta Metall.* 36(1): 1–12.
25. Huang, X., Chaturvedi, M. C., and Richards, N. L. 1996. *Metall. Trans. A* 27A: 785–790.
26. Chen, W., Chaturvedi, M. C., and Richards, N. L. 2001. *Metall. Trans. A* 32A: 931–939.
27. Morimer, M.A. 1974. Grain boundary in engineering materials, *4th Bolton Landing Conf.* J. L. Walter, J. H. Westbrook, and D. A. Woodford, eds. Claitors Publication Division, Baton Rouge, La., p. 647.
28. Guo, H., Chaturvedi, M. C., Richards, N. L., and McMahon, G. 1999. *Scripta Materialia* 40 (3): 383–388.
29. Thompson, R. G., Cassimus, J. J., Mayo, D. E., and Dobbs, J. R. 1985. *Welding Journal* 64: 91-s to 96-s.
30. Faulkner, R. G. 1981. *J. Mater. Sci.* 16: 373.
31. Nakkalil, R., Richards, N. L., and Chaturvedi, M. C. 1993. *Acta Metall. Mater.* 41 (12): 3381–3392.
32. Patterson, B. R., and Liu, Y. 1992. *Metall. Trans. A*23A: 2481.
33. Thompson, R. G. 1993. Welding metallurgy of nonferrous high temperature materials. *ASM Handbook* Vol. 6: 567.